 doi:10.20944/preprints202205.0407.v1

Article

Transcriptome Analysis of Fusarium-Tomato Interaction Based on an Up-Dated Genome Annotation of Fusarium Oxysporum F. Sp. Lycopersici Identifies Novel Effector Candidates that Suppress or Induce Cell Death in Nicotiana Benthamiana

Xizhe Sun[1,2,3], Xiangling Fang[4], Dongmei Wang[1,3], David A. Jones[2*], Lisong Ma[1,2,5*]

[1] State Key Laboratory of North China Crop Improvement and Regulation, Hebei Agricultural University, Baoding 071001, China
[2] Division of Plant Science, Research School of Biology, the Australian National University, ACT 2601, Australia
[3] Hebei Key Laboratory of Plant Physiology and Molecular Pathology, College of Life Science, Hebei Agricultural University, Baoding 071001, China.
[4] State Key Laboratory of Grassland Agro-ecosystems, Key Laboratory of Grassland Livestock Industry Innovation, Ministry of Agriculture and Rural Affairs, College of Pastoral Agriculture Science and Technology, Lanzhou University, Lanzhou 730020, China
[5] College of Horticulture, Hebei Agricultural University, Baoding 071001, China.
* Correspondence: Em. Prof. David Jones,david.jones@anu.edu.au;Dr. Lisong Ma, lisong.ma@anu.edu.au

Abstract: Fusarium oxysporum f. sp. lycopersici (Fol) causes vascular wilt disease in tomato. Upon colonization of the host, Fol secretes many small effector proteins into the xylem sap to facilitate infection. Besides known SIX (Secreted In Xylem) proteins, the identity of additional effectors that contribute to Fol patho-genicity remains largely unexplored. We have performed a deep RNA-sequencing analysis of Fol race 2-infected tomato, used the sequence data to annotate a published genome assembly generated via PacBio SMRT sequencing of the Fol race 2 reference strain Fol4287, and analysed the resulting transcriptome to identify Fol effector candidates among the newly annotated genes. We examined the Fol-infection expres-sion profiles of all 13 SIX genes present in Fol race 2 and identified 27 new candidate effector genes that were likewise significantly upregulated upon Fol infection. Using Agrobacterium-mediated transfor-mation, we tested the ability of 22 of the new candidate effector genes to suppress or induce cell death in leaves of Nicotiana benthamiana. One effector candidate designated Fol-EC19, encoding a secreted guanyl-specific ribonuclease, was found to trigger cell death and two effector candidates designated Fol-EC14 and Fol-EC20, encoding a glucanase and a secreted trypsin, respectively, were identified that can suppress Bax-mediated cell death. Remarkably, Fol-EC14 and Fol-EC20 were also found to suppress I-2/Avr2- and I/Avr1-mediated cell death. Using the yeast secretion-trap screening system, we showed that these three biologically-active effector candidates each contain a functional signal peptide for protein secretion. Our findings provide a basis for further understanding the virulence functions of Fol effectors.

Keywords: Fusarium; tomato; novel effector candidates; cell death; *Nicotiana benthamiana*

1. Introduction

Plants continuously face biotic stresses associated with fungal pathogens. To combat fungal infections, plants have evolved multiple cell-surface and intracellular receptors able to perceive pathogen molecules and activate plant immune responses (Zhou & Zhang, 2020). Conversely, adapted fungal pathogens must avoid or suppress plant immune responses to establish compatible infections (Lo Presti et al., 2015). One of the strategies employed by fungal pathogens is the secretion of effectors that can suppress plant im-mune responses and manipulate plant cell physiology to facilitate infection and fungal

 doi:10.20944/preprints202205.0407.v1

proliferation (Gi-raldo & Valent, 2013, Lo Presti et al., 2015). However, some effectors can be recognized by plant recep-tors to activate effector-triggered immunity (ETI) (Lo Presti et al., 2015, van der Burgh & Joosten, 2019). ETI often results in a rapid and localized cell death that can impede the proliferation of biotrophic fungal pathogens(Thomma et al., 2011). In turn, fungal pathogens have evolved strategies to avoid ETI via genet-ic changes in effector genes (also termed Avr or avirulence genes) recognized by corresponding R (re-sistance) genes in the host or to suppress ETI by deploying other effectors. For example, the hemibi-otrophic fungal pathogen Leptosphaeria maculans has been shown to use AvrLm3 and AvrLm5-9 effectors to suppress race-specific resistance mediated by Rlm4-7, which perceives the intracellularly localized AvrLm4-7 effector (Blondeau et al., 2015, Plissonneau et al., 2016, Ghanbarnia et al., 2018). The wheat powdery mildew effector SvrPm3a1/f1 suppresses Pm3-mediated race-specific resistance triggered by the distantly-related AvrPm3s (Bourras et al., 2015). Similarly, the Fusarium oxysporum f. sp. lycopersici Avr1 effector contributes to pathogenicity by suppressing resistance mediated by the I-2 and I-3 R proteins (Houterman et al., 2008). Nine wheat rust effectors have been shown to suppress the cell-death response caused by the transient co-expression of different Avr/R gene combinations in Nicotiana benthamiana, im-plying a possible role in suppressing ETI (Ramachandran et al., 2017).

Large-scale identification of putative fungal effectors remains challenging due to a lack of sequence con-servation among known fungal effectors. However, the availability of fungal genome sequences and RNA-seq techniques have facilitated high throughput and accurate identification of putative effectors, thereby accelerating our understanding of the molecular interactions between plants and pathogens (Selin et al., 2016). Comprehensive and enhanced bioinformatics pipelines have been developed to successfully predict effector candidates from plant pathogen genomes. For example, a bioinformatics pipeline was used to identify 725 candidate effectors from the genome and infection transcriptome of the flax rust pathogen Melampsora lini (Nemri et al., 2014). With a similar strategy and additional selection criteria, 78 effector candidates were identified from the necrotrophic plant pathogen Sclerotinia sclerotiorum (Guyon et al., 2014). Similarly, 80 effector candidates were identified via a transcriptomic analysis of the hemibi-otrophic fungal pathogen Leptosphaeria maculans during colonization of Brassica napus cotyledons (Had-dadi et al., 2016) and 32 during infection of Arabidopsis thaliana by Plasmodiophora brassicae (Perez-Lopez et al., 2020).

Unlike bacterial effectors, large-scale determinations for the virulence roles of putative fungal effectors remain limited owing to the difficulties in obtaining sufficient or multiple gene knockout mutants (Kanja & Hammond-Kosack, 2020). Because host cell death plays an important role in plant-pathogen interaction, identification of effectors with the ability to suppress or induce cell death has been of long-standing inter-est. Agrobacterium-mediated transient expression in planta has been demonstrated as an effective high-throughput tool to rapidly identify fungal proteins with the ability to suppress host cell death associated with plant immunity or to induce cell death (Petre et al., 2016). Cell death triggered by the pro-apoptotic mouse protein Bax in plants represents a similar defense-related cell-death response (Lacomme & Santa Cruz, 1999). Suppression of Bax-induced cell death by co-expression of effectors in N. benthamiana with Bax has been widely used as an efficient screening tool to identify many putative fungal effectors (Wang et al., 2011, Haddadi et al., 2016, Wang et al., 2020, Cheng et al., 2017, Ramachandran et al., 2017, Xu et al., 2019, Dutra et al., 2020, Zhang et al., 2020). A growing number of fungal effectors have also been found to induce cell death by transient expression in planta, and they can be initially considered “elicitors” or “toxins” or potential avirulence determinants recognized by plant resistance proteins (Derevnina et al., 2016, Li et al., 2020b). However, their roles in plant-fungal interactions remain controversial.

Fusarium oxysporum f. sp. lycopersici (Fol) is a soil-borne hemibiotrophic fungal pathogen that causes vascular wilt of tomato and severe yield losses in tomato production (Takken & Rep, 2010). Fol enters the tomato root through natural wounds or by direct

 doi:10.20944/preprints202205.0407.v1

penetration of epidermal cells. Following colonization of the root, Fol invades the xylem where it produces microconidia and rapidly proliferates to spread through-out the xylem. The accumulation of fungal biomass results in typical wilt disease symptoms (Olivain et al., 2006). Because the xylem serves as the primary interface between the host and pathogen, 14 small se-creted Fol proteins (<25 kDa), named SIX (Secreted In Xylem) proteins, have been identified in the xylem sap of Fol-infected tomato plants by proteomic analysis (Rep et al., 2004, Houterman et al., 2007, Schmidt et al., 2013). Most of the SIX genes are located on Fol pathogenicity chromosome 14 (Ma et al., 2010, Schmidt et al., 2013, Li et al., 2020a). Knockout mutants of five SIX genes, namely SIX1 (Avr3) (Rep et al., 2004), SIX2(Gawehns et al., 2015), SIX3 (Houterman et al., 2009), SIX5 (Ma et al., 2015) and SIX6 (Gawehns et al., 2014), are compromised in pathogenicity on susceptible tomato plants, showing that they are required for virulence. Further studies showed that complete loss of the long arm of chromosome 14, containing SIX6/9/11, and part of the short arm, including SIX7/10/12, did not abolish Fol pathogenicity (Vlaardingerbroek et al., 2016, Li et al., 2020a). Recently, a conserved SIX8-PSE1 (Pair with SIX Eight 1) gene pair in F. oxysporum isolates infecting Arabidopsis was found to suppress phytoalexin-based im-munity (Ayukawa et al., 2021). A PSE1 homolog designated PSL1 (PSE1-like 1) has also been found paired with SIX8 in Fol (Ayukawa et al., 2021). PSL1 also encodes a small secreted protein likely to be se-creted into the xylem of Fol-infected tomato plants.

Currently, four resistance genes have been introgressed into commercial tomato cultivars to protect against Fol infection and they have been named I (for Immunity), I-2, I-3 and I-7 (Gonzalez-Cendales et al., 2016). Avr2 (Six3) is recognized by the intracellular coiled-coil nucleotide-binding leucine-rich repeat (CC-NB-LRR) receptor I-2 (Simons et al., 1998, Houterman et al., 2009), whereas Avr1 (Six4) and Avr3 (Six1) are recognized by the cell-surface receptors I (a LRR receptor protein; LRR-RP) and I-3 (an S-receptor-like kinase; SRLK), respectively (Rep et al., 2004, Houterman et al., 2008, Catanzariti et al., 2015, Catanzariti et al., 2017). Heterologous co-expression of I-2/Avr2 triggers cell death in N. bentham-iana and tomato (Houterman et al., 2009). Similarly, heterologous co-expression of I/Avr1 triggers cell death in N. benthamiana (Catanzariti et al., 2017). The arms race between Fol and tomato results in the emergence of new pathogenic races able to overcome the resistance conferred by I genes, and is driven by evolutionary adaption of Fol effector genes to the host (Takken & Rep, 2010, Jenkins et al., 2021). There-fore, the discovery of novel Fol effectors is required to completely understand the virulence mechanisms evolved by Fol and counter this threat. Newly identified effectors can be utilized as probes to identify new resistance genes or to determine susceptibility loci in vulnerable crops (Vleeshouwers & Oliver, 2014, Domazakis et al., 2017).

To identify new effectors contributing to Fol virulence and obtain a comprehensive expression profile of known SIX genes and new effector candidates during Fol infection, we performed a genome-wide tran-scriptomic analysis to identify genes encoding small secreted proteins upregulated during infection of to-mato at 2, 4, and 6 days post inoculation (dpi). We identified 40 effector candidates and obtained expres-sion profiles for known SIX genes and novel effector candidates. We validated the secretion signal peptide of selected effector candidates and characterized the ability of effector candidates to suppress Bax-, Avr2/I-2- and Avr1/I-induced cell death in N. benthamiana. In addition, we examined their ability to induce cell death in N. benthamiana. Our findings provide strong evidence that some of the new effector candi-dates contribute to Fol pathogenicity.

2. Materials and Methods

Plant material and growth conditions

 doi:10.20944/preprints202205.0407.v1

The tomato cultivar Moneymaker, which is susceptible to all Fol races, was used in this study. Money-maker seedlings were germinated and grown in a growth chamber with 22°C, 16 h days (100 µE m−2 sec−1) and 18°C, 8 h nights. Nicotiana benthamiana plants were grown in a growth chamber at 25°C with a 16 h (100 µE m−2 sec−1) day length.

Fol strain and inoculations

Fol race 2 isolate Fol007 (carrying Avr2 and Avr3) was used in this study. Ten-day-old Moneymaker seed-lings were inoculated with Fol spores according to the root dip method (Mes et al., 1999). After inocula-tion, the plants were kept in a growth chamber at 22°C with a 16 h day length as described above. .

Extraction of RNA for RNA-seq and qRT-PCR analysis

For RNA extraction, mock- or Fol-inoculated Moneymaker seedlings were grown on vermiculite supple-mented with nutrients. The roots of six plants per treatment at 2, 4, and 6 dpi were harvested and frozen in liquid nitrogen. This experiment was repeated three times to generate biological replicates. For RNA ex-traction from mycelium, Fol007 mycelia were grown in minimal growth medium (3% w/v sucrose, 1% w/v KNO3, and 0.17% w/v yeast nitrogen base without amino acids or ammonia) at 25°C and 175 rpm for five days, and mycelium was collected, quickly dried and frozen in liquid nitrogen. RNA was extracted as described previously (Haddadi et al., 2016). Briefly, six roots per sample or 1 mg of mycelium were ground in liquid nitrogen. The ground samples were extracted using TRIzol LS reagent (Invitrogen, Carls-bad, USA) and purified using the PureLink™ RNA Mini Kit following the manufacturer's instructions (Invitrogen). DNA was removed with PureLink DNase Set (Invitrogen) using the on-column approach. RNA was quantified by a Qubit fluorometer (Invitrogen) and checked for quality by an Agilent Bioanalyzer 2100 (Agilent Technologies, Santa Clara, California, USA) following the manufacturer's protocol. Sam-ples with integrity numbers above 8.0 were used for RNA-seq.

For qRT-PCR analysis, cDNA was synthesized using the iScript™ cDNA Synthesis Kit (Bio-Rad, Hercu-les, California, USA). qRT-PCR primers were designed using Primer-Blast (Wu et al., 2013)

(Ye et al., 2012) and checked against the Fol genome for specificity (Table S1). qRT-PCR was performed using Applied Biosystems ViiA™ 7 Real-Time PCR System (Applied Biosystems, Waltham, Massachu-setts, USA) and SYBR Green Master Mix (Applied Bio-systems). The Fol ACTIN gene was used as a refer-ence. Quantification of relative gene expression levels was performed using the 2-△△Ct method (Rao et al., 2013).

RNA-seq-guided genome annotation and genome alignment

RNA-seq libraries were prepared and sequenced by Novogene (Beijing, China) using a HiSeq 2500 plat-form (Illumina, Inc., San Diego, USA). To predict and annotate genes, we aligned RNA-seq reads to the recent assembly of the Fol4287 genome generated by SMRT (single molecule real time) PacBio sequenc-ing (GCA_001703175.2;(Li et al., 2020a)) using HISAT2.2 (Kim et al., 2019). Scallop v0.10.4 (Shao & Kingsford, 2017) was used to assemble the paired reads into transcripts. All assembled transcripts were used for gene prediction by CodingQuarry v2.0 (-d parameter) (Testa et al., 2015) and aligned reads were used for gene prediction by BRAKER v2.1.6 with nondefault parameters--fungus--species= “fusari-um_oxysporum” (Hoff et al., 2019). These two gene prediction outputs were combined using funannotate pipeline v 1.8.7 (https://github.com/nextgenusfs/funannotate/) which passes the combined gene predictions onto EVidenceModeler v.1.1.1 to generate a consensus annotation of protein-coding genes (https://zenodo.org/record/4054262#.X8MXPM0zaHs). The completeness of gene prediction was exam-ined using BUSCO v.5.2.1 (benchmarking universal single-copy ortholog) with the “fungi_odb10” library (Waterhouse et al., 2018).

 doi:10.20944/preprints202205.0407.v1

MCScanX toolkit was used to distinguish between collinear and lineage-specific (LS) regions in the Fol 4287 genome assembly generated via SMRT PacBio sequencing (GCA_001703175.2) relative to the F. verticillioides (Fv) genome (Wang et al., 2012). Chromosome regions with at least ten orthologous gene pairs shared between the Fol genome and Fv genomes were identified as collinear. Orthologous genes were identified via BLASTp with an E-value cut-off of 1e−10 (Johnson et al., 2008).

The 4287 genome assembly generated via SMRT PacBio sequencing (GCA_001703175.2) was aligned with the previous 4287 genome assembly generated via Sanger sequencing (GCA_000149955.2;(Ma et al., 2010)) using MUMmer 3.23 with --maxmatch (Kurtz et al., 2004). LS regions, the locations of candidate effector genes and the relationship between the two genome assemblies were visualized via Circos plots constructed using Advanced Circos in TBtools (Chen et al., 2020).

Secretome prediction

The pipeline used in this study for the prediction of the Fol secretome was modified from previous studies (Nemri et al., 2014, Haddadi et al., 2016, Neu & Debener, 2019). Briefly, SignalP 5.0 (Armenteros et al., 2019) was used to predict signal peptides with a cut-off of 0.8. Mature protein sequences (with signal pep-tides removed) were used as inputs for TMHMM v2.0c (Krogh et al., 2001) to identify proteins with transmembrane domains, which were then removed. All protein sequences remaining after this step were checked by TargetP 1.1 (Emanuelsson et al., 2000) to remove proteins targeted to mitochondria. ScanPro-site (de Castro et al., 2006) was then used to remove proteins targeted to the endoplasmic reticulum. Final-ly, PredGPI (Pierleoni et al., 2008) was used to remove proteins with glycosylphosphatidylinositol anchors with a false positive rate ≤ 0.01.

Gene expression analysis

The expression of newly assembled transcripts, including transcripts from the original genome annotation that were present in the predicted secretome, were quantified via Salmon 1.5.1 (Patro et al., 2017), which was set with the argument KeepDuplicates in the indexing step and validateMappings and --numBootstraps 100 in the quantification step. Differential gene expression analysis was performed using the Bioconductor package DESeq2 v. 1.6.3 (Love et al., 2014) by comparing the gene expression at different time points in Fol007-inoculated samples with gene expression in the mycelium sample. Clustered heatmaps showing the expression profiles of candidate effector genes were generated using TBtools (Chen et al., 2020).

Plant transformation vector construction

To generate constructs for transient expression in N. benthamiana, 22 effector candidate genes were ampli-fied using primers listed in Supplementary Table S1. The resulting PCR products were cloned into the in-house ligation-independent cloning (LIC) vector pSL, which was derived from pGreenII (Hellens et al., 2005) and carries a CaMV 35S promoter and tobacco PR1a signal peptide sequence, using the protocol de-scribed previously (De Rybel et al., 2011). The resulting pSL:effector-candidate-gene constructs were used for Agrobacterium transformation as described previously (Ma et al., 2012).

Agrobacterium-mediated transient assays in N. benthamiana

Agrobacterium-mediated transient transformation of N. benthamiana was performed according to methods described previously (Ma et al., 2012). Briefly, Agrobacterium cultures were grown to an absorbance of 0.8 at 600 nm in LB-mannitol medium supplemented with 20 μM acetosyringone and 10 mM MES pH 5.6. Cells were pelleted by centrifugation at 2800 × g for 20 min and then resuspended in infiltration medium (10 mM MES pH 5.6, 2% w/v sucrose, 200 μM acetosyringone) to an absorbance at 600 nm of 1.

 doi:10.20944/preprints202205.0407.v1

Infiltra-tions were conducted on leaves of 4-5-week old N. benthamiana plants. The resulting responses were pho-tographed 5 days after infiltration.

Yeast secretion trap assay

The predicted coding sequences of the signal peptides of selected effector candidates were amplified from cDNA using the primers listed in Table S1 and cloned into the yeast secretion trap vector pSUC2 using EcoRI and XhoI restriction sites. The signal peptide coding sequence of N. benthamiana pathogenesis-related protein 1a (PR1a) was also cloned into pSUC2 for use as a positive control. The resulting con-structs were transformed into the yeast strain YTK12 to examine secretion following the method described previously (Ma et al., 2018, Yin et al., 2018). Briefly, yeast transformants able to grow on selective CMD-W media (6.7 g yeast nitrogen base without amino acids, 20 g sucrose, 1 g glucose and 0.74 g minus tryp-tophan dropout supplement in 1000 ml distilled water with 15 g agar) (Yin et al., 2018) were transferred to fresh CMD-W and YPRAA plates (1% w/v yeast extract, 2% w/v peptone, 2% w/v raffinose, and 2 μg/mL antimycin A). The secretory function of a putative signal peptide is determined by the growth of colonies on YPRAA plates after 3 days incubation at 30 °C and the reduction of colorless 2,3,5-triphenyltetrazolium chloride (TTC) to red-colored insoluble triphenylformazan as described by Yin et al. (Yin et al., 2018)

3. Results

Identifying candidate effector genes expressed during Fol infection

To identify novel Fol effector candidates expressed during Fol infection, we performed RNA-seq analysis using RNA samples prepared from Moneymaker tomato plants at 2, 4 and 6 dpi with Fol race 2 and from mycelium grown in vitro. The Fol 4287 reference genome was recently re-sequenced using PacBio SMRT sequencing to improve the quality of the genome sequence and assembly (Li et al., 2020a). We aligned the previous Fol4287 genome assembly (GCA_000149955.2; (Ma et al., 2010)) based on Sanger sequencing, here designated the Fol 2010 genome, with the newly assembled genome (GCA_001703175.2), here desig-nated the Fol 2020 genome, and found the assembly of LS chromosomes differed markedly between the two assemblies (Fig. S1 and S2). Based on this observation, we decided to map RNA-seq reads to the Fol 2020 genome. For RNA samples prepared from Fol infected tomato, 80-97 million raw reads were pro-duced and after filtering out small reads 0.35-1.31 million paired-end reads were mapped to the Fol 2020 genome accounting for 0.39%-1.35% of the reads (Table S2). For RNA prepared from Fol growing in vitro, a total of 30.2 million raw reads were produced and 29.2 million paired-end reads were mapped to the Fol 2020 genome. Next, we annotated the Fol 2020 genome using our RNA-seq data, resulting in 26,826 gene models (Table S3). Genome annotation quality was assessed using the BUSCO tool, which produced 751 complete, three fragmented and four missing BUSCOs from a total of 758 BUSCO groups based on the fungi_obd10 database, resulting in a 99.5% BUSCO completeness score (Table S4). The annotated pro-tein-coding sequences were assigned FOXGR gene IDs and used to search against the old Fol 2010 prote-ome. Identical sequences with their old FOXG gene IDs were also listed (Table S3). In total, 26,826 pre-dicted proteins were used as the basis for the prediction of the Fol secretome.

Based on the effector prediction pipelines employed previously for other plant pathogens and the charac-teristics of known effectors of plant pathogenic fungi, e.g. less than 300 amino acids in length (Nemri et al., 2014, Haddadi et al., 2016, Sperschneider et al., 2018, Neu & Debener, 2019), a bioinformatics pipe-line was adopted to identify the Fol effector candidates expressed during infection (Fig. 1). This pipeline involved three main processes; preparation of a Fol proteome, secretome prediction and effector predic-tion (Fig. 1). As shown in Fig.1, 1312 proteins were identified with a signal peptide and no

 doi:10.20944/preprints202205.0407.v1

transmembrane domain consistent with secretion via the classical secretory pathway. After removing proteins predicted to target the ER or mitochondria, and GPI anchored proteins, a total of 1119 proteins were included in the predicted Fol 2020 secretome, accounting for 4.17% of the predicted Fol 2020 proteome. Of these 1119 proteins, 532 were ≤300 amino acids and of these 77 proteins were encoded by genes that were significant-ly up-regulated at 2, 4 and 6 dpi during Fol infection in comparison to their expression in mycelium, in-cluding all of the SIX genes present in Fol race 2. As SIX13 exhibited the lowest transcript per million (TPM) values among all SIX genes at 2, 4 and 6 dpi, we selected 55 secreted-protein-coding genes that had TPM values equal to or greater than that of SIX13 at each time point as a set of Fol effector candidates (Table 1). These included two identical copies of SIX13 and eight identical copies each of SIX8 and PSL1, leaving a non-redundant total of 40 candidate effectors. Next, the sequence annotations of these candidate effector genes were validated by the alignment of reads to the reference genome.

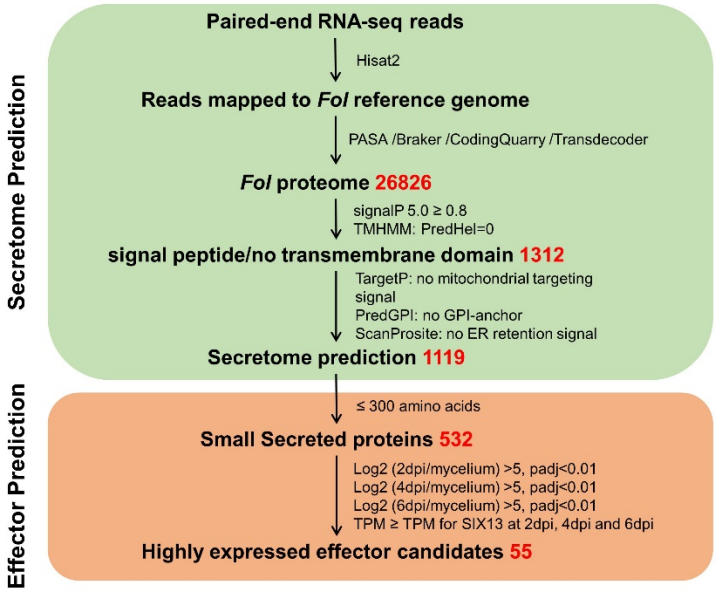

Figure 1. Bioinformatic pipeline for the prediction of *Fol* effector candidates. Two main steps are included in this pipeline: Prediction of the *Fol* secretome based on transcripts aligned to the PacBio-sequenced reference genome Fol4287 and identification of *Fol* genes encoding small secreted proteins differentially-expressed during *Fol* infection. Based on the expression profile of the *SIX13* gene, which had the lowest transcript per million (TPM) value among the 13 SIX genes present in *Fol* race 2, 55 genes were selected as effector candidates.

Preprints (www.preprints.org) | NOT PEER-REVIEWED | Posted: 31 May 2022 doi:10.20944/preprints202205.0407.v1

Table 1. Characteristics of 55 effector candidates with TPM values greater than or equal to that of *SIX13* during *Fol* infection.

Name.	Lineage-specific region	Chromo-some	2020 contig	Start	End	Strand	In-trons	Pro-tein length	Cys-teine resi-dues	Protein do-main/homol-ogy
SIX9	YES	14	14	809946	810290	-	0	114	6	
SIX6	YES	14	14	962344	963070	-	1	225	9	
SIX11	YES	14	14	1007574	1007906	-	0	110	8	
FOXG_17276*	YES	14	14	1450230	1450661	-	0	143	6	LysM domain
PSL2*	YES	14	14	1486868	1487339	-	3	106	9	PSE1 homo-logue
SIX14	YES	14	14	1489136	1489452	+	1	88	6	
SIX1	YES	14	14	1508020	1508874	-	0	284	8	
SIX2	YES	14	14	1515507	1516205	+	0	232	8	
SIX3	YES	14	14	1620196	1620687	-	0	163	3	
SIX5	YES	14	14	1621885	1622410	+	3	119	7	
SIX13	YES	14	14	1721250	1722191	+	1	293	12	
SIX10	YES	14	14	1929603	1930122	-	1	149	2	
SIX12	YES	14	14	1931346	1931777	-	1	127	10	
SIX7	YES	14	14	1934097	1934727	+	1	163	2	
FOXGR_015522	YES	14	14	1996473	1996874	-	2	79	9	
SIX13	YES	14	14	2018772	2019713	+	1	293	12	
FOXGR_015533*	YES	14	14	2033852	2034196	-	0	114	3	
FOXG_10949*	NO	1	0	498344	498719	-	1	107	8	hydrophobin
FOXG_10950*	NO	1	0	500457	501074	+	3	152	9	hydrophobin
FOXG_11033*	NO	1	0	722540	723369	-	3	226	0	
FOXG_05750	NO	2	53	540805	541602	+	0	265	12	LysM domain x2
FOXG_05755*	NO	2	53	549873	550346	+	0	157	3	
FOXG_18699*	NO	4	2	3264675	3264965	+	0	96	10	
FOXGR_007323*	NO	5	3	2372326	2372640	-	1	86	0	
FOXG_10672	NO	7	46	413827	414423	+	0	198	13	PAN/Apple do-main x2
FOXG_04863*	NO	7	46	3884224	3885126	+	0	300	8	

Preprints (www.preprints.org) | NOT PEER-REVIEWED | Posted: 31 May 2022 doi:10.20944/preprints202205.0407.v1

FOXG_04805*	NO	7	46	4051134	4051586	+	1	132	8	
FOXG_02829*	NO	8	50	561065	561514	-	0	149	16	
FOXGR_021626*	NO	8	50	3119908	3120893	+	2	294	3	glucanase – Fol-EC14
SIX8	YES	8	50	4122866	4123541	-	2	141	2	
PSL1*	YES	8	50	4124187	4124677	+	3	111	9	
FOXG_08899*	NO	9	5	3212288	3212782	+	1	148	1	
SIX8	YES	10	7	1363	1768	+	2	141	2	
FOXGR_010884	NO	10	7	444492	445286	+	0	264	0	
FOXG_11745*	NO	10	7	655322	655924	+	1	183	4	phospholipase A2
SIX8	YES	10	7	3412328	3413003	-	2	141	2	
PSL1*	YES	10	7	3413649	3414139	+	3	111	9	
FOXG_10138	NO	11	61	398337	399122	+	0	261	2	peptidase G1 family
FOXGR_025639*	NO	11	61	507487	507728	+	1	61	2	
FOXG_16600*	NO	11	61	2173630	2174176	-	1	164	0	
FOXG_13233*	NO	12	12	668427	668929	+	2	131	4	ribonuclease F1 – Fol-EC19
FOXG_13248*	NO	12	12	703080	703929	+	2	248	6	trypsin – Fol-EC20
FOXG_14607*	NO	12	12	1873367	1874245	+	1	275	7	metalloprote-ase MEP1
FOXG_14684*	NO	12	12	2089656	2090270	-	2	168	14	
PSL1*	YES	–	9	576	1066	-	3	111	9	
SIX8	YES	–	10	224	783	+	2	141	2	
PSL1*	YES	–	44	18988	19478	-	3	111	9	
SIX8	YES	–	44	20124	20683	+	2	141	2	
PSL1*	YES	–	45	6024	6515	-	3	111	9	
PSL1*	YES	–	58	1499796	1500286	-	3	111	9	
SIX8	YES	–	58	1500932	1501607	+	2	141	2	
PSL1*	YES	–	59	3963	4453	-	3	111	9	
SIX8	YES	–	59	5099	5658	+	2	141	2	
PSL1*	YES	–	60	7085	7575	--	3	111	9	
SIX8	YES	–	60	8221	8896	+	2	141	2	

Table 1. Characteristics of 55 effector candidates with TPM values greater than or equal to that of SIX13 during Fol infection.

* Novel candidate effector genes that were tested for cell-death induction and suppression of Bax-induced cell death in N. benthamiana.

Preprints (www.preprints.org) | NOT PEER-REVIEWED | Posted: 31 May 2022 doi:10.20944/preprints202205.0407.v1

In addition, we generated Circos plots to visualise the chromosomal distribution of Fol effector candidates. As shown in Fig. 2A, 22 effector candidates are located on Fv-collinear regions of the 11 core chromo-somes in the Fol genome. However, effector candidate FOXGR_025639 had no ortholog in Fv despite hav-ing orthologs in other Fusarium species including F. graminearum. Four of these 22 effector candidates, FOXGR_007323, FOXGR_010884, FOXGR_021626 and FOXGR_025639, were either not predicted or predicted incorrectly in the annotation of the Fol 2010 genome assembly. As shown in Fig. 2B, 33 effector candidates were located in LS regions compared to the Fv genome, most on chromosome 14. Two SIX8/PSL1 gene pairs and one lone copy of SIX8 were located in LS regions near the ends of core chromo-somes 8 and 10 in the Fol 2020 assembly, one SIX8/PSL1 gene pair on contig 58, a large chromosome-sized contig similar to LS chromosome 3 in the Fol 2010 genome assembly, and three SIX8/PSL1 gene pairs, one lone copy of SIX8 and two lone copies of PSL1 on small unpositioned contigs (Fig. 2). Four new effector candidates were identified on chromosome 14, including FOXGR_015533, which was completely absent from the Fol 2010 genome sequence, FOXGR_015322 (a homologue of PSE1 here designated PSL2), which was not predicted in the annotation of the Fol 2010 genome assembly, and FOXGR_015522, which was predicted incorrectly. All 13 of the SIX genes present in Fol race 2 and PSL1 were identified in the Fol 2020 assembly, whereas SIX7, SIX8, SIX10, SIX11, SIX12 and PSL1 were either not predicted or predicted incorrectly in the annotation of the Fol 2010 genome assembly.

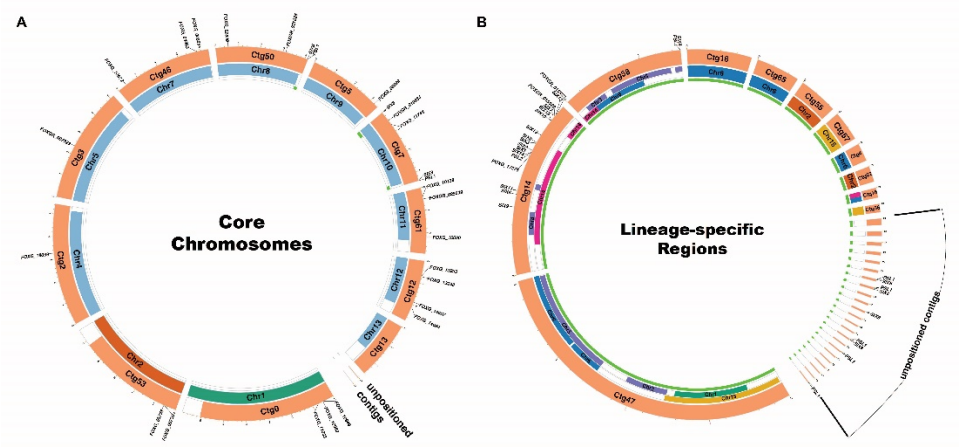

Figure 2. Distribution of the 55 *Fol* effector candidate genes on the physical map of the Fol4287 genome. Circos plots showing the distributions of *Fol* effector candidate genes on the core chromosomes (**A**) and the lineage-specific (LS) regions (**B**). Circles from inside to outside represent the LS regions in *Fol* (shown in green) compared to the *Fov* genome, the core chromosomes or LS regions of Fol4287 assembled following Sanger sequencing (shown in various colours) and corresponding contigs assembled following PacBio sequencing (shown in orange). .

Expression profiles of Fol effector candidates during infection

To explore the expression profiles of Fol effector candidates upon infection, we performed a hierarchical-clustering heatmap analysis of the 40 non-redundant effector candidates using their TPM values. Fig. 3A shows that they grouped into four clusters correlated with their expression at three different Fol infection time points. Cluster 1 contains genes that were highly up-regulated at 2 dpi but less so at 4 and 6 dpi. Clus-ter 2 represents genes that were highly up-regulated at 2 and 6 dpi but less so at at 4 dpi. All 13 SIX genes were included in cluster 3, which contains genes up-regulated progressively from 2 to 6 dpi. Genes in clus-ter 4 were highly up-regulated at 4 dpi, but less so at 2 and 6 dpi. Our results indicate that all identified Fol effector candidate genes exhibit high expression upon Fol infection and that candidates in clusters 2 and 3, which were

Preprints (www.preprints.org) | NOT PEER-REVIEWED | Posted: 31 May 2022 doi:10.20944/preprints202205.0407.v1

most up-regulated at 6 dpi, might play important roles during Fol infection given that all SIX genes that contribute to Fol pathogenicity were highly up-regulated at 6 dpi.

To validate the quantitative gene expression detected in the RNA-seq analysis (Fig. 3B), a total of ten dif-ferentially expressed effector candidates, including two or three genes from each cluster, were selected for validation. Their relative expression levels at 2, 4, and 6 dpi were quantified by qRT-PCR. The qRT-PCR expression profiles of all ten genes confirmed their upregulation during infection and seven of the ten showed similar patterns of expression to those evident from the RNA-seq data (Fig. 3B).

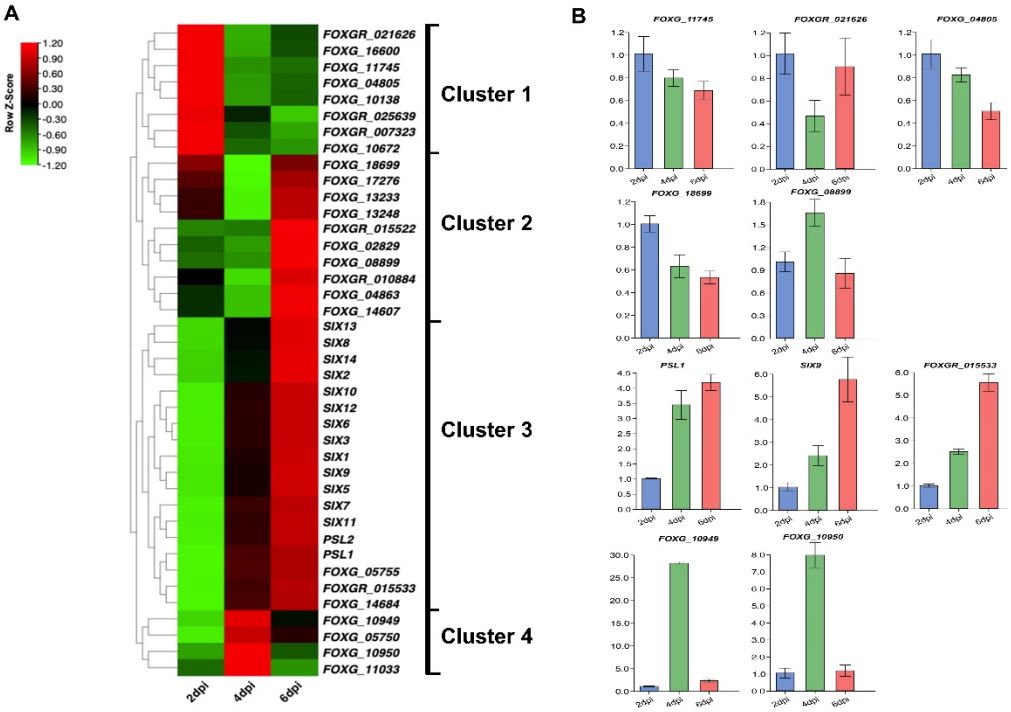

Figure 3. Expression profiles of effector candidate genes and validation of the expression of selected effector candidate genes during *Fol* infection by RT-qPCR.

A). Clustered heatmaps of the 40 *Fol* differentially-expressed effector candidate genes at 2, 4 and 6 dpi based on RNA-seq data. The row color scale reflects the values of log2 (mean TPM) at each timepoint), in which red represents higher expression and green represents lower expression. Genes are grouped into four clusters with distinct expression profiles over the three-time points. **B).** Quantitative RT-PCR analysis showing the expression of effector candidate genes selected from each cluster in infected tomato roots at 2, 4 and 6 dpi. *Fol* actin was used as an internal reference gene and expression levels were normalized to actin. Values are means of three independent biological samples and error bars represent standard deviations.

Identification of cell death-inducing effector candidates

Host cell death is a hallmark of defense against a biotrophic fungal pathogen, but could contribute to path-ogenicity for a hemi-biotrophic pathogen like Fol. To identify effector candidates inducing cell death, 22 effector candidate genes were selected for cloning and transient expression via agroinfiltration of N. ben-thamiana leaves (Table S5). GFP was used as a negative control and Bax was used as a positive control in these experiments. We found that one of the 22 effector candidates, Fol-EC19, triggered cell death at 3 dpi (Fig. 4). In addition, we used RT-PCR to show that all 22 candidate genes were expressed in N. bentham-iana. (Fig. S3).

Preprints (www.preprints.org) | NOT PEER-REVIEWED | Posted: 31 May 2022 doi:10.20944/preprints202205.0407.v1

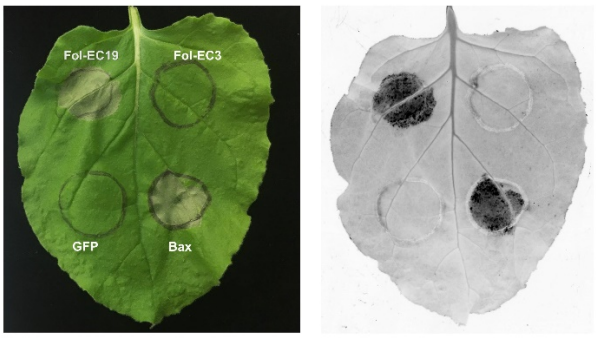

Figure 4. *Fol-EC19* induces cell death in the leaves of *N. benthamiana*. *N. benthamiana* leaves were agro-infiltrated with a construct containing the *Fol-EC19* effector candidate gene. *GFP* and *Fol-EC3* served as negative controls and *Bax* served as a positive control. Representative leaves were photographed 3 days after infiltration and the experiment was repeated at least three times with consistent results.

Identification of effector candidates that suppress Bax-induced cell death using a transient expression assay

Many fungal effectors suppress host cell-death to facilitate pathogen infection (Coll et al., 2011). To iden-tify effector candidates that can suppress Bax-induced cell death, we co-agroinfiltrated N. benthamiana leaves with Bax and each of the remaining 21 effector genes used for the cell-death experiments described above. GFP was used as a negative control. Bax triggers rapid cell death in N. benthamiana leaves at 2 dpi (Fig. 5). Fol-EC14 and Fol-EC20 were found to completely suppress Bax-induced cell death whereas leaf re-gions co-expressing GFP and Bax developed pronounced cell death (Fig. 5).

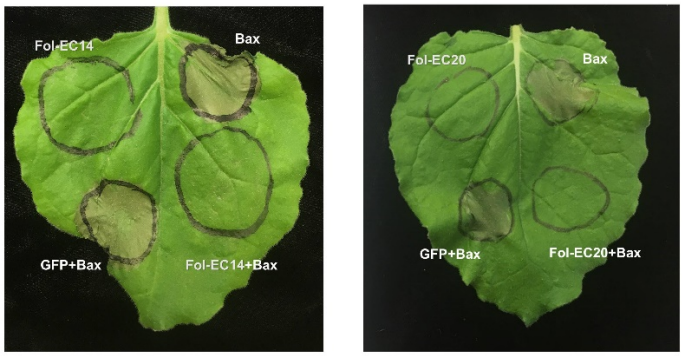

Figure 5. Fol-EC14 and Fol-EC20 can suppress Bax-induced cell death. *A. tumefaciens* carrying either *Fol-EC14* or *Fol-EC20* effector candidate gene was infiltrated into *N. benthamiana* leaves, followed 24 hours later by infiltration with *A. tumefaciens* carrying the *Bax* gene. *GFP* served as a negative control. Representative leaves were photographed 3 days after infiltration and the experiment was repeated at least three times with consistent results.

Suppression of I/Avr1- and I-2/Avr2-induced cell death

To investigate whether Fol-EC14 and Fol-EC20 function as suppressors of cell death triggered by tomato proteins conferring Fol-resistance, we transiently co-expressed Fol-EC14 and Fol-EC20 with I/Avr1 or I-2/Avr2 in N. benthamiana leaves, using GFP as a negative control. No cell death was observed in leaf re-gions co-expressing Fol-EC14 or Fol-EC20 with I/Avr1 or I-2/Avr2 (Fig. 6). In contrast, co-expression of I/Avr1 or I-2/Avr2 with GFP triggered rapid cell death at 3 dpi. These findings indicated that Fol-EC14 and Fol-EC20 inhibited cell death triggered by both a CC-NB-LRR resistance protein (I-2 in this instance) and an LRR-RP resistance protein (I in this instance).

 doi:10.20944/preprints202205.0407.v1

Figure 6. Fol-EC14 and Fol-EC20 can suppress cell death triggered by Fusarium-wilt resistance genes. *A. tumefaciens* carrying either *Fol-EC14* or *Fol-EC20* effector candidate gene was infiltrated into *N. benthamiana* leaves followed 24 hours by co-infiltration with *A. tumefaciens* carrying the *Avr1* and *I* or *Avr2* and *I-2* genes. *GFP* served as a negative control. Representative leaves were photographed 3 days after infiltration and the experiment was repeated at least three times with consistent results.

To further explore whether Fol-EC14 and Fol-EC20 are able to suppress cell death triggered by other plant R genes, we transiently co-expressed them with L6TIR in N. benthamiana leaves. The TIR (Toll Interleu-kin-1 Receptor) domain of the flax L6 TIR-NB-LRR resistance protein is able to homodimerize in the ab-sence of its NB and LRR domains to trigger plant cell death (Bernoux et al., 2011) L6TIR-induced cell death was not inhibited by either Fol-EC14 or Fol-EC20 (Fig. S4). In addition, we examined their ability to suppress Fol-EC19-induced cell death. Neither Fol-EC14 nor Fol-EC20 was able to suppress cell death induced by Fol-EC19 (Fig. S4).

Functional characterization of the signal peptides of the Fol-EC14, Fol-EC19, and Fol-EC20 effectors

To examine the function of the predicted signal peptide sequences of Fol-EC14, Fol-EC19 and Fol-EC20, a yeast signal sequence trap system was employed. The predicted signal peptide coding sequences of Fol-EC14, Fol-EC19 and Fol-EC20 were amplified and cloned in frame with a truncated SUC2 gene, which encodes yeast invertase lacking its signal peptide. The resulting constructs and positive control pSUC2::SPPR1a (carrying the N. benthamiana PR1a signal-peptide coding sequence) were transformed into yeast strain YKT12, which cannot grow on medium without a simple sugar due to a deficiency of the yeast invertase gene. Consistent with the positive control, YTK12 strains carrying the predicted signal peptide sequences of Fol-EC14, Fol-EC19 and Fol-EC20 fused to SUC2 were able to grow on YPRAA plates (Fig. 7). As expected, they were also able to catalyze the conversion of colorless TTC to red-colored TFP (Fig. 7). Conversely, the negative control (YTK12 with empty vector) was not able to grow on a YPRAA plate and did not induce a TTC to TFP color change (Fig. 7). These results demonstrated that the predicted sig-nal peptides of Fol-EC14, Fol-EC19 and Fol-EC20 are functional.

 doi:10.20944/preprints202205.0407.v1

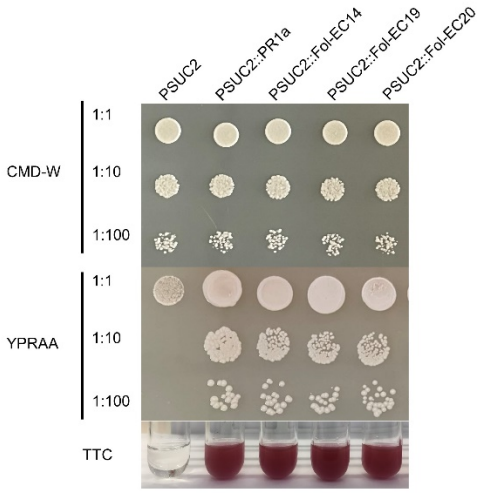

Figure 7. Yeast secretion trap assay of the predicted signal peptides of cell-death inducing and cell-death suppressing effector candidates. The predicted signal peptide coding sequences of *Fol-EC14*, *Fol-EC19* and *Fol-EC20* were cloned into the yeast secretion-trap vector pSUC2. The tobacco PR1a signal peptide was used as a positive control empty vector was used as a negative control. CMD-W (-Trp) was used to select the transformed yeast YTK12 carrying the pSUC2 vector. Yeast growing on the YPRAA medium indicate secretion of invertase via a functional signal peptide. Conversion of the dye 2, 3, 5-triphenyltetrazolium chloride (TTC) to the insoluble red colored triphenylformazan is also indicative of invertase secretion.

4. Discussion

The effectors secreted by plant pathogenic fungi determine the outcome of infection by either suppressing plant immune response or interfering with plant physiological processes to facilitate pathogen infection (Lo Presti et al., 2015, Hogenhout et al., 2009, Lievens et al., 2009). The study presented here identified a repertoire of newly assembled Fol transcripts and 40 non-redundant effector candidates whose expression is highly induced during tomato infection, including all 13 SIX genes present in Fol race 2. Functional analysis of 22 of the 27 novel effector candidates revealed that one effector candidate induced cell death and two effector candidates suppressed R-protein-mediated cell death. We further demonstrated that these three effector candidates have a functional signal peptide. Together, these findings enrich the genome an-notation of Fol, deliver genome-wide expression profiles of genes encoding small secreted protein includ-ing the SIX genes, and provide a basis for further exploring Fol pathogenic mechanisms.

Previously, annotation of the published Fol reference genome was based on gene prediction without tran-scriptome analysis (Ma et al., 2010). Thus, inevitable inaccuracies occurred and some still remain. For ex-ample, several SIX genes, including SIX7, SIX8, SIX11, SIX12 and SIX14 were not annotated in the refer-ence genome, but were subsequently submitted as separate NCBI accessions (Schmidt et al., 2013). We have been able to assemble 26,826 transcripts from transcriptome sequencing data mapped to a genome assembly based on PacBio SMRT genome sequencing (Fig. 1), including all of the previously unannotated SIX genes. In addition, eight effector candidate genes were identified that were absent from the Fol 2010 reference genome annotation (Table 1). Of the non-redundant total of 40 candidate effector genes, 18, in-cluding all 13 SIX genes present in Fol race 2 , are located on LS regions and the remaining 22 on core regions (Table 1 and Fig. 2). Importantly, three of the newly annotated genes, PSL2, FOXGR_015522 and FOXGR_015533, and one previously annotated gene, FOXG_17276 are located on the LS pathogenicity chromosome 14, providing a strong indication that they might be involved in Fol infection. Multiple cop-ies of SIX8 and the newly annotated PSL1 gene are located

 doi:10.20944/preprints202205.0407.v1

in other LS regions, mostly as divergently-oriented pairs (Table 1 and Fig. 2). None of the 18 candidate LS effectors had homologs with known func-tion, although FOXG_17276 has a LysM domain suggesting a role in carbohydrate binding. In contrast, eight of the 22 candidate core region effectors had homology to proteins of known function, including two hydrophobins, a glucanase, a phospholipase, a ribonuclease and three proteases (Table 1). Cell-wall-degrading, membrane-attacking and proteolytic enzymes are well-known parts of a plant pathogen's arse-nal and it is not surprising that degradative enzymes falling below the 300 amino acid threshold should be captured by this analysis as potential effectors. However, roles for a glucanase and trypsin in suppression of defence-related cell death and a ribonuclease in the induction of cell death were unexpected.

FOXGR_021626, here designated Fol-EC14, encodes a glucanase containing a GH131 glycosyl hydrolase domain, which was first described in the ascomycete Podospora anserina as PaGluc131A (Lafond et al., 2012) and in the basidiomycete Coprinopsis cinerea as CcGH131A (Miyazaki et al., 2013). PaGluc131A has been reported to have β-1,3- and β-1,6-exoglucanase and β-1,4 endoglucanase activities (Lafond et al., 2012), and a later study also reported β-1,3-endoglucanase activity, but could not confirm β-1,6-exoglucanase activity (Anasontzis et al., 2019). Despite comprising almost entirely a GH131 domain, Fol-EC14 only has 23% and 24% amino acid sequence identity with the N-terminal glycosyl hydrolase do-mains of PaGluc131A and CcGH131A, respectively. GH131 proteins are widespread among the Ascomy-cota and Basidiomycota and an extensive phylogenetic analysis has identified two clades each containing ascomycete and basidiomycete sequences suggesting divergence of the two GH131 clades prior to the di-vergence of the Ascomycota from the Basidiomyota (Anasontzis et al., 2019). Fol-EC14 falls in one clade and PaGluc131A and CcGH131A fall in the other. Interestingly, Fusarium is completely absent from the PaGluc131A/CcGH131A clade although other members of the Sordariomycetes are represented in both (Fig. S5 and S6).

Two members of the Fol-EC14 clade, Colletotrichum higginsianum ChGluc131A and ChGluc131B (Fig. S7and S8), have also been shown to have β-1,3-exoglucanase, and β-1,3- and β-1,4 endoglucanase activities (Anasontzis et al., 2019). Fol-EC14 and ChGluc131B and most of their orthologs lack three of the four res-idues thought to be important for PaGluc131A and CcGH131A catalytic activity (Miyazaki et al., 2013), whereas ChGluc131A and its orthologs lack only one of these residues (Fig. S6, S7and S8). They also dif-fer from members of the PaGluc131A/CcGH131A clade by the presence of two conserved cysteine resi-dues flanking the GH131 domain, which could potentially form a stabilizing disulphide bond (Figs. S6, S7 and S8). Fol-EC14 has only 43% sequence identity with ChGluc131A and 48% with ChGluc131B, which in turn have only 43% sequence identity with one another. Consistent with these differences, Fol-EC14, ChGluc131A and ChGluc131B are each member of distinct phylogenetic subgroups within the Fol-EC14 clade (Fig. S6, S7 and S8), with ChGluc131B and its orthologs limited to the genus Colletotrichum (Fig. S8)., and Fusarium sequences present only in the Fol-EC14 subgroup (Fig. S6). Like Fol-EC14, ChGluc131B lacks three of the four residues thought to be important for PaGluc131A and CcGH131A catalytic activity, but is nevertheless catalytically active. This suggests a different mechanism of catalysis to that proposed for PaGluc131A and CcGH131A, but given the absence of information about residues im-portant for ChGluc131B catalysis and the low sequence identity between Fol-EC14 and ChGluc131B, we cannot infer whether Fol-EC14 is catalytically active or not. If it were functional, possible roles for Fol-EC14 could include degradation of cellulose (β-1,4 glucan) in the plant cell wall, callose (β-1,3 glucan) degradation, conversion of elicitor-active glucans to shorter elicitor-inactive oligomers, and exoglucanase-mediated release of glucose as a nutrient for the fungus.

FOXG_13248, here designated Fol-EC20, encodes a secreted trypsin that differs by a single conservative amino-acid substitution from a structurally and enzymatically well-characterized F. oxysporum trypsin (Schmidt et al., 2003, Rypniewski et al., 1993). Trypsins are widespread among plant pathogens, as are trypsin inhibitors among plant hosts.

 doi:10.20944/preprints202205.0407.v1

In the xylem-colonising gram-positive bacterium Clavibacter michi-ganensis subsp. michiganensis (Cmm), two genes, pat-1 and chpC, encode secreted trypsin-family proteins that are required for colonisation and wilting of tomato, and suppression of the plant immune response (Stork et al., 2008, Chalupowicz et al., 2017). Interestingly, Cmm also requires a β-1,4 endoglucanase en-coded by the celA gene for pathogenicity and wilting of tomato (Jahr et al., 2000). Potentially, the Fol-EC14 exo/endoglucanase and Fol-EC20 trypsin might play similar roles in Fol pathogenicity.

There are three possible explanations for the suppression of Bax-induced and R-protein-induced cell death by Fol-EC14 and Fol-EC20, for which there may be some precedents. One explanation might be that en-zymatic actions of Fol-EC14 or Fol-EC20 suppress plant cell death. Sanchez et al. (1992) reported that wa-ter-soluble glucans from Phytophthora infestans can suppress fungal-elicitor-induced plant cell death (Sanchez et al., 1992), and Ali et al. (2015) reported that a potato cyst nematode expansin could suppress NPP (Nep1-like protein) and CNL-induced cell death (Ali et al., 2015). Expansins are plant cell-wall loos-ening proteins. Given these two observations, it is plausible that either a soluble glucan product of Fol-EC14 catalysis or the effect of Fol-EC14 catalysis on the plant cell wall could have a suppressive effect on plant cell death. Similalry, Carlile et al. (2000) reported that the Stagonospora nodorum trypsin SNP1 re-leased hydroxyproline from wheat cell walls, and, like β-1,4 endoglucanases, contributes to modification of the plant cell wall (Carlile et al., 2000). Hao et al. (2019) reported that a specific F. graminearum arabi-nanase, albeit a different glycosyl hydrolase to Fol-EC14, could suppress Bax-induced cell death (Hao et al., 2019). Given that the arabinanase could also suppress flg22- and chitin-induced ROS (reactive oxygen species) production, they inferred that the suppression of Bax-induced cell death was likely related to the suppression of ROS production. A later study by the same group showed that a putative endoglucanase from F. graminearum could suppress chitin-induced but not flg22-induced ROS production (Hao et al., 2020). No explanation for the mechanisms involved in the suppression of ROS production was provided by either study and, although the products of arabinanase or endoglucanase catalysis could be involved, a di-rect effect of the arabinanase or endoglucanse protein could not be excluded. A key question that therefore remains to be answered is whether the catalytic activities of Fol-EC14 and Fol-EC20 are required for their suppressive effects.

A second explanation might be that the Fol-EC14 or Fol-EC20 proteins have a direct effect on plant cell death unrelated to enzymatic function. Rose et al. identified non-catalytic members of the trypsin family in Phytophthora as inhibitors of plant β-1,3 endoglucanases able to reduce the production of elicitor-active oligoglucans from the Phytophthora cell wall (Rose et al., 2002). Potentially, this inhibition could promote the production of water-soluble glucans able to suppress fungal-elicitor-induced plant cell death as de-scribed above. A third explanation is that the suppression of cell death by Fol-EC14 and Fol-EC20 is an artifact. Bozkurt et al. suggest that heterologous expression of some proteins can elicit an unfolded protein response in the ER that can suppress Bax-induced cell death (Bozkurt et al., 2012). Given that Fol-EC14 and Fol-EC20 have been targeted to the plant ER as part of the secretory pathway, it is possible that they do not fold properly and thereby elicit an unfolded protein response in the ER. However, the fact that they were not able to suppress either L6TIR- or Fol-Ec19-induced cell death suggests this is not the explanation (Fig. S4).

FOXG_13233, here designated Fol-EC19, encodes a secreted guanyl-specific ribonuclease that induces ra-ther than suppresses plant cell death in N. benthamiana (Fig. 4). Homologs of Fol-EC19 are widely dis-tributed among the fungi including plant pathogens in the genera Alternaria, Bipolaris, Colletotrichum, Fusarium, Magnaporthe, Pyrenophora, Ustilago and Verticillium. Our finding is consistent with a recent study showing that F. graminearum secretes Fg12, a ribonuclease with 85% identity and 93% similarity to Fol_EC19, that contributes to virulence on soybean as demonstrated by gene knockout experiments and induces cell death in N. benthamiana, N. tabacum and tomato as shown

by agroinfiltration experiments (Yang et al., 2021). Agroinfiltration of a mutant Fg12 gene was used to show that induction of cell death in N. benthamiana was dependent on protein secretion and ribonuclease activity. Recombinant F. gramine-arum Fg12 protein was found to induce ion leakage and PR-gene expression in N. benthamiana and re-sistance to F. graminearum and Phytophthra sojae in soybean hypocotyls, again dependent on ribonuclease activity. Whether the cell death induced by Fol-EC19 is dependent on ribonuclease activity and whether Fol-EC19 is capable of inducing plant cell death or plant immune responses in tomato remain unknown, but seems likely. These findings suggest that Fol-EC19might, like Fg12, also function as a virulence factor in the context of pathogen infection but trigger a plant immune response when tested in isolation.

Supplementary Materials:

The following supporting information can be downloaded at: www.mdpi.com/xxx/s1,Table S1. Primers used in this study;Table S2. Summary of RNA-seq statistics for three replicates of three infection time points (2, 4 and 6 dpi) and mycelium grown *in vitro*;Table S3. List of predicted proteins encoded by genes annotated from the PacBio-sequenced Fol4287 genome assembly; Table S4. Summary comparison of the Fol4287 genome assemblies and annotations obtained with Sanger and PacBio sequencing platforms. Figure S1: Whole-genome synteny analysis of predicted genes between Sanger-sequenced Fol4287 (Fol2010) and PacBio-sequenced Fol4287 (Fol2020) assemblies; Figure S2: Whole-genome alignment between Sanger-sequenced Fol4287 (Fol2010) and PacBio-sequenced Fol4287 (Fol2020); Figure S3: RT-PCR to check the expression of 22 cloned effector candidate genes in agroinfiltrated N. benthamiana leaves; Figure S4: FolEC-14 and Eol-EC20 are not able to inhibit L6TIR- and Fol-EC19-induced cell death in N. benthamiana leaves; Figure S5: PaGluc131A alignment; Figure S6: Fol-EC14 alignment; Figure S7: ChGluc131A alignment; Figure S8: ChGluc131B alignment.

Funding

This research was funded by the Australian Research Council (ARC) through Discovery Early Career Researcher Award (DE170101165) to L. Ma. X. Sun was supported by the scholarship under the Hebei Agricultural University (No. 20190002) and China Scholarship Council (No. 202008130203) for stay at the Australian National University.

Author Contributions

Conceptualization, L.M. and D.J.; methodology, X.S., X. F. and L.M.; writing—original draft preparation, X.S., L.M. and D.J.; writing—review and editing, L.M. and D.J.; supervision, D.J., L.M. and D.W.; project administration, L.M.; funding acquisition, L.M. All authors have read and agreed to the published version of the manuscript.

Data Availability Statement

The data that support the findings of this study are available from the corresponding author upon request and RNA-seq data are available in NCBI BioProject ID: PRJNA841073.

Conflicts of Interest

The authors declare no conflict of interest.

References

1. Ali, S., Magne, M., Chen, S., Cote, O., Stare, B. G., Obradovic, N., *et al.* (2015) Analysis of putative apoplastic effectors from the nematode, Globodera rostochiensis, and identification of an expansin-like protein that can induce and suppress host defenses. *PLoS One,* **10,** e0115042.
2. Anasontzis, G. E., Lebrun, M. H., Haon, M., Champion, C., Kohler, A., Lenfant, N., *et al.* (2019) Broad-specificity GH131 beta-glucanases are a hallmark of fungi and oomycetes that colonize plants. *Environ Microbiol,* **21,** 2724-2739.
3. Armenteros, J. J. A., Tsirigos, K. D., Sonderby, C. K., Petersen, T. N., Winther, O., Brunak, S., *et al.* (2019) SignalP 5.0 improves signal peptide predictions using deep neural networks. *Nature Biotechnology,* **37,** 420-+.
4. Ayukawa, Y., Asai, S., Gan, P., Tsushima, A., Ichihashi, Y., Shibata, A., *et al.* (2021) A pair of effectors encoded on a conditionally dispensable chromosome of Fusarium oxysporum suppress host-specific immunity. *Commun Biol,* **4,** 707.
5. Bernoux, M., Ve, T., Williams, S., Warren, C., Hatters, D., Valkov, E., *et al.* (2011) Structural and functional analysis of a plant resistance protein TIR domain reveals interfaces for self-association, signaling, and autoregulation. *Cell Host Microbe,* **9,** 200-211.

6. Ali, S., Magne, M., Chen, S., Cote, O., Stare, B. G., Obradovic, N., *et al.* (2015) Analysis of putative apoplastic effectors from the nematode, Globodera rostochiensis, and identification of an expansin-like protein that can induce and suppress host defenses. *PLoS One,* **10,** e0115042.
7. Anasontzis, G. E., Lebrun, M. H., Haon, M., Champion, C., Kohler, A., Lenfant, N., *et al.* (2019) Broad-specificity GH131 beta-glucanases are a hallmark of fungi and oomycetes that colonize plants. *Environ Microbiol,* **21,** 2724-2739.
8. Armenteros, J. J. A., Tsirigos, K. D., Sonderby, C. K., Petersen, T. N., Winther, O., Brunak, S., *et al.* (2019) SignalP 5.0 improves signal peptide predictions using deep neural networks. *Nature Biotechnology,* **37,** 420-+.
9. Ayukawa, Y., Asai, S., Gan, P., Tsushima, A., Ichihashi, Y., Shibata, A., *et al.* (2021) A pair of effectors encoded on a conditionally dispensable chromosome of Fusarium oxysporum suppress host-specific immunity. *Commun Biol,* **4,** 707.
10. Bernoux, M., Ve, T., Williams, S., Warren, C., Hatters, D., Valkov, E., *et al.* (2011) Structural and functional analysis of a plant resistance protein TIR domain reveals interfaces for self-association, signaling, and autoregulation. *Cell Host Microbe,* **9,** 200-211.
11. Blondeau, K., Blaise, F., Graille, M., Kale, S. D., Linglin, J., Ollivier, B., *et al.* (2015) Crystal structure of the effector AvrLm4-7 of Leptosphaeria maculans reveals insights into its translocation into plant cells and recognition by resistance proteins. *Plant J,* **83,** 610-624.
12. Bourras, S., McNally, K. E., Ben-David, R., Parlange, F., Roffler, S., Praz, C. R., *et al.* (2015) Multiple Avirulence Loci and Allele-Specific Effector Recognition Control the Pm3 Race-Specific Resistance of Wheat to Powdery Mildew. *The Plant cell,* **27,** 2991-3012.
13. Bozkurt, T. O., Schornack, S., Banfield, M. J. and Kamoun, S. (2012) Oomycetes, effectors, and all that jazz. *Curr Opin Plant Biol,* **15,** 483-492.
14. Carlile, A. J., Bindschedler, L. V., Bailey, A. M., Bowyer, P., Clarkson, J. M. and Cooper, R. M. (2000) Characterization of SNP1, a cell wall-degrading trypsin, produced during infection by Stagonospora nodorum. *Mol Plant Microbe Interact,* **13,** 538-550.
15. Catanzariti, A. M., Do, H. T., Bru, P., de Sain, M., Thatcher, L. F., Rep, M., *et al.* (2017) The tomato I gene for Fusarium wilt resistance encodes an atypical leucine-rich repeat receptor-like protein whose function is nevertheless dependent on SOBIR1 and SERK3/BAK1. *Plant J,* **89,** 1195-1209.
16. Catanzariti, A. M., Lim, G. T. T. and Jones, D. A. (2015) The tomato I-3 gene: a novel gene for resistance to Fusarium wilt disease. *New Phytol,* **207,** 106-118.
17. Chalupowicz, L., Barash, I., Reuven, M., Dror, O., Sharabani, G., Gartemann, K. H., *et al.* (2017) Differential contribution of Clavibacter michiganensis ssp. michiganensis virulence factors to systemic and local infection in tomato. *Mol Plant Pathol,* **18,** 336-346.
18. Chen, C. J., Chen, H., Zhang, Y., Thomas, H. R., Frank, M. H., He, Y. H., *et al.* (2020) TBtools: An Integrative Toolkit Developed for Interactive Analyses of Big Biological Data. *Mol Plant,* **13,** 1194-1202.
19. Cheng, Y., Wu, K., Yao, J., Li, S., Wang, X., Huang, L., *et al.* (2017) PSTha5a23, a candidate effector from the obligate biotrophic pathogen Puccinia striiformis f. sp. tritici, is involved in plant defense suppression and rust pathogenicity. *Environ Microbiol,* **19,** 1717-1729.
20. Coll, N. S., Epple, P. and Dangl, J. L. (2011) Programmed cell death in the plant immune system. *Cell Death Differ,* **18,** 1247-1256.
21. de Castro, E., Sigrist, C. J. A., Gattiker, A., Bulliard, V., Langendijk-Genevaux, P. S., Gasteiger, E., *et al.* (2006) ScanProsite: detection of PROSITE signature matches and ProRule-associated functional and structural residues in proteins. *Nucleic Acids Research,* **34,** W362-W365.
22. De Rybel, B., van den Berg, W., Lokerse, A., Liao, C. Y., van Mourik, H., Moller, B., *et al.* (2011) A versatile set of ligation-independent cloning vectors for functional studies in plants. *Plant Physiol,* **156,** 1292-1299.
23. Derevnina, L., Dagdas, Y. F., De la Concepcion, J. C., Bialas, A., Kellner, R., Petre, B., *et al.* (2016) Nine things to know about elicitins. *New Phytol,* **212,** 888-895.
24. Domazakis, E., Lin, X., Aguilera-Galvez, C., Wouters, D., Bijsterbosch, G., Wolters, P. J., *et al.* (2017) Effectoromics-Based Identification of Cell Surface Receptors in Potato. In: *Plant Pattern Recognition Receptors: Methods and Protocols.* (Shan, L. and He, P., eds.). New York, NY: Springer New York, pp. 337-353.
25. Dutra, D., Agrawal, N., Ghareeb, H. and Schirawski, J. (2020) Screening of Secreted Proteins of Sporisorium reilianum f. sp. zeae for Cell Death Suppression in Nicotiana benthamiana. *Front Plant Sci,* **11,** 95.
26. Emanuelsson, O., Nielsen, H., Brunak, S. and von Heijne, G. (2000) Predicting subcellular localization of proteins based on their N-terminal amino acid sequence. *J Mol Biol,* **300,** 1005-1016.
27. Gawehns, F., Houterman, P. M., Ichou, F. A., Michielse, C. B., Hijdra, M., Cornelissen, B. J., *et al.* (2014) The Fusarium oxysporum effector Six6 contributes to virulence and suppresses I-2-mediated cell death. *Mol Plant Microbe Interact,* **27,** 336-348.
28. Gawehns, F., Ma, L., Bruning, O., Houterman, P. M., Boeren, S., Cornelissen, B. J., *et al.* (2015) The effector repertoire of Fusarium oxysporum determines the tomato xylem proteome composition following infection. *Front Plant Sci,* **6,** 967.
29. Ghanbarnia, K., Ma, L., Larkan, N. J., Haddadi, P., Fernando, W. G. D. and Borhan, M. H. (2018) Leptosphaeria maculans AvrLm9: a new player in the game of hide and seek with AvrLm4-7. *Mol Plant Pathol,* **19,** 1754-1764.
30. Giraldo, M. C. and Valent, B. (2013) Filamentous plant pathogen effectors in action. *Nat Rev Microbiol,* **11,** 800-814.
31. Gonzalez-Cendales, Y., Catanzariti, A. M., Baker, B., McGrath, D. J. and Jones, D. A. (2016) Identification of I-7 expands the repertoire of genes for resistance to Fusarium wilt in tomato to three resistance gene classes. *Mol Plant Pathol,* **17,** 448-463.
32. Guyon, K., Balague, C., Roby, D. and Raffaele, S. (2014) Secretome analysis reveals effector candidates associated with broad host range necrotrophy in the fungal plant pathogen Sclerotinia sclerotiorum. *BMC Genomics,* **15,** 336.

33. Haddadi, P., Ma, L., Wang, H. and Borhan, M. H. (2016) Genome-wide transcriptomic analyses provide insights into the lifestyle transition and effector repertoire of Leptosphaeria maculans during the colonization of Brassica napus seedlings. *Mol Plant Pathol,* **17,** 1196-1210.
34. Hao, G., McCormick, S., Usgaard, T., Tiley, H. and Vaughan, M. M. (2020) Characterization of Three Fusarium graminearum Effectors and Their Roles During Fusarium Head Blight. *Front Plant Sci,* **11,** 579553.
35. Hao, G., McCormick, S., Vaughan, M. M., Naumann, T. A., Kim, H. S., Proctor, R., *et al.* (2019) Fusarium graminearum arabinanase (Arb93B) Enhances Wheat Head Blight Susceptibility by Suppressing Plant Immunity. *Mol Plant Microbe Interact,* **32,** 888-898.
36. Hellens, R. P., Allan, A. C., Friel, E. N., Bolitho, K., Grafton, K., Templeton, M. D., *et al.* (2005) Transient expression vectors for functional genomics, quantification of promoter activity and RNA silencing in plants. *Plant Methods,* **1,** 13.
37. Hoff, K. J., Lomsadze, A., Borodovsky, M. and Stanke, M. (2019) Whole-Genome Annotation with BRAKER. *Methods in molecular biology,* **1962,** 65-95.
38. Hogenhout, S. A., Van der Hoorn, R. A. L., Terauchi, R. and Kamoun, S. (2009) Emerging Concepts in Effector Biology of Plant-Associated Organisms. *Molecular Plant-Microbe Interactions,* **22,** 115-122.
39. Houterman, P. M., Cornelissen, B. J. and Rep, M. (2008) Suppression of plant resistance gene-based immunity by a fungal effector. *PLoS Pathog,* **4,** e1000061.
40. Houterman, P. M., Ma, L., van Ooijen, G., de Vroomen, M. J., Cornelissen, B. J., Takken, F. L., *et al.* (2009) The effector protein Avr2 of the xylem-colonizing fungus Fusarium oxysporum activates the tomato resistance protein I-2 intracellularly. *Plant J,* **58,** 970-978.
41. Houterman, P. M., Speijer, D., Dekker, H. L., CG, D. E. K., Cornelissen, B. J. and Rep, M. (2007) The mixed xylem sap proteome of Fusarium oxysporum-infected tomato plants. *Mol Plant Pathol,* **8,** 215-221.
42. Jahr, H., Dreier, J., Meletzus, D., Bahro, R. and Eichenlaub, R. (2000) The endo-beta-1,4-glucanase CelA of Clavibacter michiganensis subsp. michiganensis is a pathogenicity determinant required for induction of bacterial wilt of tomato. *Mol Plant Microbe Interact,* **13,** 703-714.
43. Jenkins, S., Taylor, A., Jackson, A. C., Armitage, A. D., Bates, H. J., Mead, A., *et al.* (2021) Identification and Expression of Secreted In Xylem Pathogenicity Genes in Fusarium oxysporum f. sp. pisi. *Frontiers in Microbiology,* **12**.
44. Johnson, M., Zaretskaya, I., Raytselis, Y., Merezhuk, Y., McGinnis, S. and Madden, T. L. (2008) NCBI BLAST: a better web interface. *Nucleic Acids Res,* **36,** W5-9.
45. Kanja, C. and Hammond-Kosack, K. E. (2020) Proteinaceous effector discovery and characterization in filamentous plant pathogens. *Mol Plant Pathol,* **21,** 1353-1376.
46. Kim, D., Paggi, J. M., Park, C., Bennett, C. and Salzberg, S. L. (2019) Graph-based genome alignment and genotyping with HISAT2 and HISAT-genotype. *Nat Biotechnol,* **37,** 907-915.
47. Krogh, A., Larsson, B., von Heijne, G. and Sonnhammer, E. L. L. (2001) Predicting transmembrane protein topology with a hidden Markov model: Application to complete genomes. *J Mol Biol,* **305,** 567-580.
48. Kurtz, S., Phillippy, A., Delcher, A. L., Smoot, M., Shumway, M., Antonescu, C., *et al.* (2004) Versatile and open software for comparing large genomes. *Genome Biol,* **5,** R12.
49. Lacomme, C. and Santa Cruz, S. (1999) Bax-induced cell death in tobacco is similar to the hypersensitive response. *Proc Natl Acad Sci U S A,* **96,** 7956-7961.
50. Lafond, M., Navarro, D., Haon, M., Couturier, M. and Berrin, J. G. (2012) Characterization of a broad-specificity beta-glucanase acting on beta-(1,3)-, beta-(1,4)-, and beta-(1,6)-glucans that defines a new glycoside hydrolase family. *Appl Environ Microbiol,* **78,** 8540-8546.
51. Li, J., Fokkens, L., Conneely, L. J. and Rep, M. (2020a) Partial pathogenicity chromosomes in Fusarium oxysporum are sufficient to cause disease and can be horizontally transferred. *Environ Microbiol,* **22,** 4985-5004.
52. Li, Y., Han, Y., Qu, M., Chen, J., Chen, X., Geng, X., *et al.* (2020b) Apoplastic Cell Death-Inducing Proteins of Filamentous Plant Pathogens: Roles in Plant-Pathogen Interactions. *Front Genet,* **11,** 661.
53. Lievens, B., Houterman, P. M. and Rep, M. (2009) Effector gene screening allows unambiguous identification of Fusarium oxysporum f. sp. lycopersici races and discrimination from other formae speciales. *FEMS Microbiol Lett,* **300,** 201-215.
54. Lo Presti, L., Lanver, D., Schweizer, G., Tanaka, S., Liang, L., Tollot, M., *et al.* (2015) Fungal effectors and plant susceptibility. *Annu Rev Plant Biol,* **66,** 513-545.
55. Love, M. I., Huber, W. and Anders, S. (2014) Moderated estimation of fold change and dispersion for RNA-seq data with DESeq2. *Genome Biol,* **15,** 550.
56. Ma, L., Houterman, P. M., Gawehns, F., Cao, L., Sillo, F., Richter, H., *et al.* (2015) The AVR2-SIX5 gene pair is required to activate I-2-mediated immunity in tomato. *New Phytol,* **208,** 507-518.
57. Ma, L., Lukasik, E., Gawehns, F. and Takken, F. L. (2012) The use of agroinfiltration for transient expression of plant resistance and fungal effector proteins in Nicotiana benthamiana leaves. *Methods in molecular biology,* **835,** 61-74.
58. Ma, L. J., van der Does, H. C., Borkovich, K. A., Coleman, J. J., Daboussi, M. J., Di Pietro, A., *et al.* (2010) Comparative genomics reveals mobile pathogenicity chromosomes in Fusarium. *Nature,* **464,** 367-373.
59. Ma, L. S., Djavaheri, M., Wang, H. Y., Larkan, N. J., Haddadi, P., Beynon, E., *et al.* (2018) Leptosphaeria maculans Effector Protein AvrLm1 Modulates Plant Immunity by Enhancing MAP Kinase 9 Phosphorylation. *Iscience,* **3,** 177-+.

60. Mes, J. J., Wit, R., Testerink, C. S., de Groot, F., Haring, M. A. and Cornelissen, B. J. (1999) Loss of Avirulence and Reduced Pathogenicity of a Gamma-Irradiated Mutant of Fusarium oxysporum f. sp. lycopersici. *Phytopathology,* **89,** 1131-1137.
61. Miyazaki, T., Yoshida, M., Tamura, M., Tanaka, Y., Umezawa, K., Nishikawa, A., *et al.* (2013) Crystal structure of the N-terminal domain of a glycoside hydrolase family 131 protein from Coprinopsis cinerea. *Febs Lett,* **587,** 2193-2198.
62. Nemri, A., Saunders, D. G., Anderson, C., Upadhyaya, N. M., Win, J., Lawrence, G. J., *et al.* (2014) The genome sequence and effector complement of the flax rust pathogen Melampsora lini. *Front Plant Sci,* **5,** 98.
63. Neu, E. and Debener, T. (2019) Prediction of the Diplocarpon rosae secretome reveals candidate genes for effectors and virulence factors. *Fungal Biol-Uk,* **123,** 231-239.
64. Olivain, C., Humbert, C., Nahalkova, J., Fatehi, J., L'Haridon, F. and Alabouvette, C. (2006) Colonization of tomato root by pathogenic and nonpathogenic Fusarium oxysporum strains inoculated together and separately into the soil. *Appl Environ Microbiol,* **72,** 1523-1531.
65. Patro, R., Duggal, G., Love, M. I., Irizarry, R. A. and Kingsford, C. (2017) Salmon provides fast and bias-aware quantification of transcript expression. *Nat Methods,* **14,** 417-+.
66. Perez-Lopez, E., Hossain, M. M., Tu, J., Waldner, M., Todd, C. D., Kusalik, A. J., *et al.* (2020) Transcriptome Analysis Identifies Plasmodiophora brassicae Secondary Infection Effector Candidates. *J Eukaryot Microbiol,* **67,** 337-351.
67. Petre, B., Saunders, D. G., Sklenar, J., Lorrain, C., Krasileva, K. V., Win, J., *et al.* (2016) Heterologous Expression Screens in Nicotiana benthamiana Identify a Candidate Effector of the Wheat Yellow Rust Pathogen that Associates with Processing Bodies. *PLoS One,* **11,** e0149035.
68. Pierleoni, A., Martelli, P. L. and Casadio, R. (2008) PredGPI: a GPI-anchor predictor. *Bmc Bioinformatics,* **9**.
69. Plissonneau, C., Daverdin, G., Ollivier, B., Blaise, F., Degrave, A., Fudal, I., *et al.* (2016) A game of hide and seek between avirulence genes AvrLm4-7 and AvrLm3 in Leptosphaeria maculans. *New Phytol,* **209,** 1613-1624.
70. Ramachandran, S. R., Yin, C., Kud, J., Tanaka, K., Mahoney, A. K., Xiao, F., *et al.* (2017) Effectors from Wheat Rust Fungi Suppress Multiple Plant Defense Responses. *Phytopathology,* **107,** 75-83.
71. Rao, X., Huang, X., Zhou, Z. and Lin, X. (2013) An improvement of the 2^(-delta delta CT) method for quantitative real-time polymerase chain reaction data analysis. *Biostat Bioinforma Biomath,* **3,** 71-85.
72. Rep, M., van der Does, H. C., Meijer, M., van Wijk, R., Houterman, P. M., Dekker, H. L., *et al.* (2004) A small, cysteine-rich protein secreted by Fusarium oxysporum during colonization of xylem vessels is required for I-3-mediated resistance in tomato. *Mol Microbiol,* **53,** 1373-1383.
73. Rose, J. K., Ham, K. S., Darvill, A. G. and Albersheim, P. (2002) Molecular cloning and characterization of glucanase inhibitor proteins: coevolution of a counterdefense mechanism by plant pathogens. *The Plant cell,* **14,** 1329-1345.
74. Rypniewski, W. R., Hastrup, S., Betzel, C., Dauter, M., Dauter, Z., Papendorf, G., *et al.* (1993) The sequence and X-ray structure of the trypsin from Fusarium oxysporum. *Protein Eng,* **6,** 341-348.
75. Sanchez, L. M., Ohno, Y., Miura, Y., Kawakita, K. and Doke, N. (1992) Host Selective Suppression by Water-Soluble Glucans from Phytophthora spp. of Hypersensitive Cell Death of Suspension-Cultures Cells from Some Solanaceous Plants Caused by Hyphal Wall Elicitors of the Fungi. *Japanese Journal of Phytopathology,* **58,** 664-670.
76. Schmidt, A., Jelsch, C., Ostergaard, P., Rypniewski, W. and Lamzin, V. S. (2003) Trypsin revisited: crystallography AT (SUB) atomic resolution and quantum chemistry revealing details of catalysis. *J Biol Chem,* **278,** 43357-43362.
77. Schmidt, S. M., Houterman, P. M., Schreiver, I., Ma, L., Amyotte, S., Chellappan, B., *et al.* (2013) MITEs in the promoters of effector genes allow prediction of novel virulence genes in Fusarium oxysporum. *BMC Genomics,* **14,** 119.
78. Selin, C., de Kievit, T. R., Belmonte, M. F. and Fernando, W. G. (2016) Elucidating the Role of Effectors in Plant-Fungal Interactions: Progress and Challenges. *Front Microbiol,* **7,** 600.
79. Shao, M. F. and Kingsford, C. (2017) Accurate assembly of transcripts through phase-preserving graph decomposition. *Nature Biotechnology,* **35,** 1167-+.
80. Simons, G., Groenendijk, J., Wijbrandi, J., Reijans, M., Groenen, J., Diergaarde, P., *et al.* (1998) Dissection of the fusarium I2 gene cluster in tomato reveals six homologs and one active gene copy. *The Plant cell,* **10,** 1055-1068.
81. Sperschneider, J., Dodds, P. N., Gardiner, D. M., Singh, K. B. and Taylor, J. M. (2018) Improved prediction of fungal effector proteins from secretomes with EffectorP 2.0. *Molecular Plant Pathology,* **19,** 2094-2110.
82. Stork, I., Gartemann, K. H., Burger, A. and Eichenlaub, R. (2008) A family of serine proteases of Clavibacter michiganensis subsp. michiganensis: chpC plays a role in colonization of the host plant tomato. *Mol Plant Pathol,* **9,** 599-608.
83. Takken, F. and Rep, M. (2010) The arms race between tomato and Fusarium oxysporum. *Mol Plant Pathol,* **11,** 309-314.
84. Testa, A. C., Hane, J. K., Ellwood, S. R. and Oliver, R. P. (2015) CodingQuarry: highly accurate hidden Markov model gene prediction in fungal genomes using RNA-seq transcripts. *BMC Genomics,* **16,** 170.
85. Thomma, B. P., Nurnberger, T. and Joosten, M. H. (2011) Of PAMPs and effectors: the blurred PTI-ETI dichotomy. *The Plant cell,* **23,** 4-15.
86. van der Burgh, A. M. and Joosten, M. (2019) Plant Immunity: Thinking Outside and Inside the Box. *Trends Plant Sci,* **24,** 587-601.
87. Vlaardingerbroek, I., Beerens, B., Rose, L., Fokkens, L., Cornelissen, B. J. and Rep, M. (2016) Exchange of core chromosomes and horizontal transfer of lineage-specific chromosomes in Fusarium oxysporum. *Environ Microbiol,* **18,** 3702-3713.
88. Vleeshouwers, V. G. and Oliver, R. P. (2014) Effectors as tools in disease resistance breeding against biotrophic, hemibiotrophic, and necrotrophic plant pathogens. *Mol Plant Microbe Interact,* **27,** 196-206.

 doi:10.20944/preprints202205.0407.v1

89. Wang, Q., Han, C., Ferreira, A. O., Yu, X., Ye, W., Tripathy, S., *et al.* (2011) Transcriptional programming and functional interactions within the Phytophthora sojae RXLR effector repertoire. *The Plant cell,* **23,** 2064-2086.
90. Wang, Y., Li, J., Xiang, S., Zhou, J., Peng, X., Hai, Y., *et al.* (2020) A putative effector UvHrip1 inhibits BAX-triggered cell death in Nicotiana benthamiana, and infection of Ustilaginoidea virens suppresses defense-related genes expression. *PeerJ,* **8,** e9354.
91. Wang, Y. P., Tang, H. B., DeBarry, J. D., Tan, X., Li, J. P., Wang, X. Y., *et al.* (2012) MCScanX: a toolkit for detection and evolutionary analysis of gene synteny and collinearity. *Nucleic Acids Research,* **40**.
92. Waterhouse, R. M., Seppey, M., Simao, F. A., Manni, M., Ioannidis, P., Klioutchnikov, G., *et al.* (2018) BUSCO Applications from Quality Assessments to Gene Prediction and Phylogenomics. *Mol Biol Evol,* **35,** 543-548.
93. Wu, H., Wang, C. and Wu, Z. (2013) A new shrinkage estimator for dispersion improves differential expression detection in RNA-seq data. *Biostatistics,* **14,** 232-243.
94. Xu, Q., Tang, C., Wang, X., Sun, S., Zhao, J., Kang, Z., *et al.* (2019) An effector protein of the wheat stripe rust fungus targets chloroplasts and suppresses chloroplast function. *Nat Commun,* **10,** 5571.
95. Yang, B., Wang, Y., Tian, M., Dai, K., Zheng, W., Liu, Z., *et al.* (2021) Fg12 ribonuclease secretion contributes to Fusarium graminearum virulence and induces plant cell death. *J Integr Plant Biol,* **63,** 365-377.
96. Ye, J., Coulouris, G., Zaretskaya, I., Cutcutache, I., Rozen, S. and Madden, T. L. (2012) Primer-BLAST: A tool to design target-specific primers for polymerase chain reaction. *Bmc Bioinformatics,* **13**.
97. Yin, W., Wang, Y., Chen, T., Lin, Y. and Luo, C. (2018) Functional Evaluation of the Signal Peptides of Secreted Proteins. *Bio Protoc,* **8,** e2839.
98. Zhang, N., Yang, J., Fang, A., Wang, J., Li, D., Li, Y., *et al.* (2020) The essential effector SCRE1 in Ustilaginoidea virens suppresses rice immunity via a small peptide region. *Mol Plant Pathol,* **21,** 445-459.
99. Zhou, J. M. and Zhang, Y. (2020) Plant Immunity: Danger Perception and Signaling. *Cell,* **181,** 978-989.